Institute of Measurement Science
Slovak Academy of Sciences

Nonlinear Prediction of Sleep Electroencephalogram

Dissertation proposal

Mgr. Kristína Šušmáková

Supervisor: RNDr. Viktor Witkovský, CSc.
Consultant: RNDr. Anna Krakovská, CSc.

2005

Contents

List of Figures

Chapter 1

Introduction

One of the most important contributions of chaos theory is the knowledge that low-dimensional deterministic systems can produce at first sight irregularly, very complicated signals and that nonlinearity is the necessary property of such systems [1]. Over the past decade chaos theory became very popular and there was a tendency to see chaos in many natural phenomena. However, one have to remain cautious about application of nonlinear techniques to data with unknown nature for it is quite easy to misinterpret the results.

Likewise, human brain and its electrical activity during various states was intensively analyzed with new nonlinear methods. First results [2] reported low-dimensional chaos during sleep with the dimension around 4, but several assumptions and details of the algorithms were not held. Additional more advanced techniques were used to resolve the question about the nature of EEG. Nor today this is definitely clarified, however, common opinion is that EEG is not purely low-dimensional chaotic system. In spite of some unresolved problems, the new nonlinear measures seem to give additional information to classical linear measures, they seem to be more successful in distinguishing between various states (e.g., sleep stages [3]) .

During sleep, human brain goes through several psychophysiological states that are relatively stable. Many nervous centres are inactive, so brain becomes a less complex system than during wakefulness and is more suitable object for mathematical modeling. The nonlinear deterministic character EEG during deep sleep was confirmed with the surrogate data test [4].

Prediction algorithms can be used to study the future, but also to investigate the dynamics of the systems; the more predictable signal - the more deterministic structure contains. Some basic prediction algorithms have been successfully applied on EEG: with respect to predictability in alpha EEG activity three various patterns were detected [5], in discrimination of evoked positive and negative emotions [6]. In current sleep research, big effort is spent on developing new systems suitable for automated scoring of sleep stages. Also the discriminatory

ability of prediction algorithms between the sleep stages can be considered.

The outline of this work is as follows. Second chapter deals with sleep and human EEG. Typical waves and patterns of sleep EEG, sleep stages, scoring rules, functions of sleep, and models of sleep regulation are described. In third section the literature review about the nature of sleep EEG is given. Some basic techniques from spectral and also nonlinear theories with their application on sleep EEG are listed. The fifth chapter contains current nonlinear prediction algorithms. And in the last two chapters the plans and aims of the next work and the description of the data are given.

Chapter 2

Sleep

2.1 Patterns and waves of EEG

EEG consists from background activity and from clearly ascendant transient phenomena [7]. The two most important characteristics of EEG elements are frequency and amplitude. Frequency is inverse value of duration of EEG element. The frequency range is divided into four bands: beta (12 Hz and higher), alpha (8-12 Hz), theta (4-8 Hz) and delta (0,1-4 Hz). Amplitude of EEG is taken as the peak to peak value. After the magnitude of amplitude EEG signal is divided into low-voltage, middle and high-voltage EEG. For delta, theta and alpha bands these values are following: 10-30 μV for low-voltage, 30-70 μV for middle-voltage and above 70 μV for high-voltage EEG. For beta band the values are lower: below 10 μV low-voltage, 10-25 μV middle-voltage and above 25 μV high-voltage EEG.

The background activity appears most of the time and is formed with four basic waves - beta, alpha, theta and delta (see Fig.2.1) or with a mixture of them. Beta activity is typical during wakefulness. Alpha occur in relaxed state with eyes closed. Theta waves are dominant in normal wake state in children, in adult people theta activity appears only in small amount especially in drowsiness. Delta waves are present in deep sleep, in healthy people do not exist in wake state. Transient phenomena characteristic for sleep are vertex waves, K - complexes and sleep spindles. Vertex wave is a sharp wave with amplitude even about 100 μV, bilateral synchronous. K complex is a sharp negative wave followed by a slower positive one. Sleep spindles are rhythmic activity in 12-14 Hz frequency range and amplitude below 50 μV.

2.2 Sleep stages

The beginning of modern sleep research dates back to the 1930s and is closely connected with the invention of the electroencephalography. In 1937, Loomis was the first to observe that

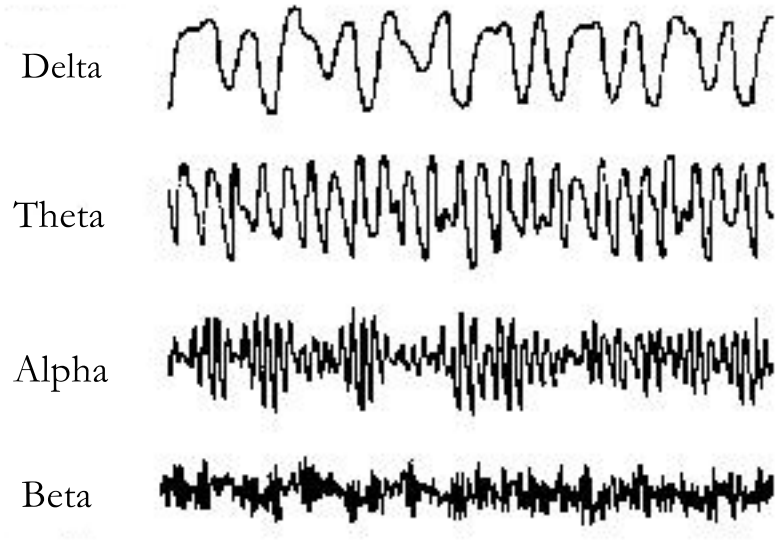

Figure 2.1: Brain waves appearing in EEG

sleep is not a homogeneous state during the whole night and he described different stages of sleep based on EEG [8]. In 1953, Aserinsky and Kleitman observed a special state of sleep - rapid eye movement (REM) sleep, during which rapid, binocularly symmetrical eye movements occur, EEG pattern is similar to the one observed during wakefulness, and both respiratory and heart rates are increased in contrast to other sleep stages. Their experiments resulted in a relationship between REM sleep and dreaming: majority of people awakened from REM sleep reported dreams, whereas people awakened during nonREM sleep did not recall dreams [9]. From overnight recording of EEG and electrooculogram (EOG), Kleitman with Dement [10] specified the cyclic pattern of REM-nonREM sleep. One cycle of REM-nonREM lasts about 90-100 minutes and during the night, 4-5 cycles occur. Aserinsky and Kleitman also divided nonREM sleep into four stages: 1 through 4, ranging from the lightest sleep in stage 1 to the deepest sleep in stage 4.

2.2.1 Rechtschaffen and Kales system

The main states of vigilance are wakefulness, REM sleep and nonREM sleep. NonREM sleep is further divided into four stages from the lightest Stage 1 to the deepest Stage 4. Stages 3 and 4 are referred to as slow wave sleep (SWS). The frequency of sleep stages alters during the night - in the early hours of sleep SWS dominates, whereas REM sleep occurs more often in the second part of sleep. The portion of REM sleep during night alters with age - in new-born babies REM sleep lasts for 50%, in adults for 20%.

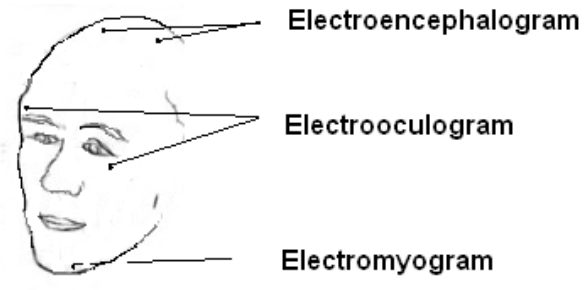

Figure 2.2: Placement of electrodes of polysomnographic measurement

An essential method in human clinical and basic sleep research is polysomnography. It is composed of measuring electroencephalogram (EEG), electrooculogram (EOG) and electromyogram (EMG) Electroencephalography is the basic method with an excellent temporal resolution and lower spatial resolution of electrical activity of cerebral cortex. The quality of EEG recording depends on some technical parameters, see [5] for details.

Sleep stages are scored according to "A Manual of Standardized Terminology, Techniques and Scoring System for Sleep stages of Human Subject", which was elaborated in 1968 by a committee co-chaired by A.Rechtschaffen and A.Kales [11]. The purpose of these uniform and standard criteria was to increase the comparability and replicability of results from different laboratories. The Manual involves parameters, techniques and wave patterns of polysomnographic recordings. One channel of EEG, two channels of EOG and one channel of EMG are recorded. The EEG derivations are C4/A1 or C3/A2 according to the 10-20 electrode placement system, see Fig. 2.3. The potentials for eyes movements recording are measured from 1 cm above and slightly lateral to the outher canthus of one eye and 1 cm below and lateral to the outer canthus of the second eye. The reference electrodes for both eyes are placed on the same ear lobe or mastoid. The EMG is recorded beneath the chin (mental, submental). The placement of electrodes of polysomnographic recording is illustrated on Fig.2.2. The stages are scored epoch-by-epoch in 20-30 s intervals.

Waking (Stage W)

There is a low voltage ($10 - 30\mu$V) and mixed frequency EEG during wakefulness (see Fig.2.4). Possible features are alpha activity in EEG and relatively high tonic EMG.

Movement Time

If in more than half an epoch of the EEG or EMG signals are unclear due to amplifier blocking or muscle activity, the epoch is counted neither with sleep nor with waking, but is labelled as movement time. It is not the same as discrete body movements, which could be

very short. Body movements can be a part of a sleep Stage or the movement time.

Stage 1

Stage 1 is characterized by low voltage, mixed frequency EEG with the highest amplitude in 2-7 Hz range (see Fig.2.4). Vertex sharp waves may occur, their amplitude can reach the value of about 200 μV. In Stage 1 after wakefulness slow eye movements can be present. The EMG level is lower than in the wakefulness. Stage 1 is also scored when the epoch is characterized with alpha activity combined with mixed frequency EEG and the amount of alpha activity is less than 50% of an epoch.

Stage 2

Stage 2 is characterized by wave patterns sleep spindles and K complexes and the absence of slow waves (see Fig.2.4). The duration of these patterns should be 0.5 s at minimum. If the time between two succeeding occurrences of sleep spindles or K complexes is lower than 3 min, this interval is scored as Stage 2, unless there are movement arousals or increased tonic activity. If the time interval is 3 min or more, it is scored as Stage 1.

Stage 3

20%-50% of the epoch of EEG record should contain waves with 2 Hz or slower and with the amplitudes above 75 μV if the epoch is scored as Stage 3, see Fig.2.4. Sleep spindles and K complexes may occur during Stage 3.

Stage 4

Stage 4 has the same attributes as Stage 3, but waves with 2 Hz and slower with the amplitudes greater than 75 μV appear more than 50% of the epoch.

Stage REM

Stage REM shows low voltage and mixed frequency (similarly to Stage 1) of EEG, sawtooth wave pattern is often present (see Fig.2.4). EMG reaches the lowest level and episodic rapid eye movements occur (REMs).

There exist cases when no movement arousals are present, EEG exhibits a relatively low voltage and mixed frequency, and sleep spindles (K complexes) characteristic for Stage 2 alternate with typical features of Stage REM (REMs, the lowest EMG level). Then scoring follows these rules:

1. Stage REM: EMG is at the lowest Stage REM level or the rapid eyes movements are

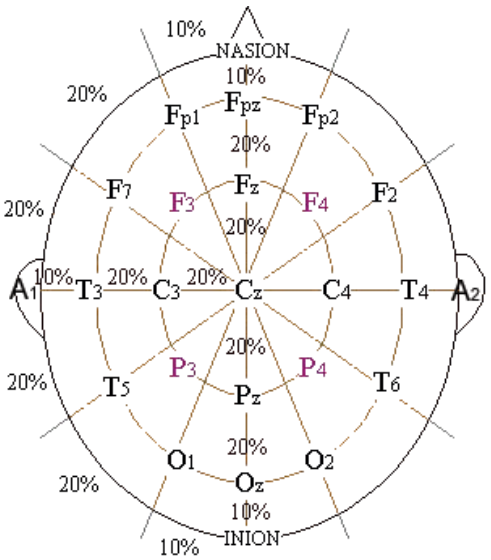

Figure 2.3: 10-20 electrode placement system for EEG measurement

present.

2. Stage 2: interval between two sleep spindles or K complexes is less than 3 minutes.

The rules of Rechtschaffen and Kales have been used for more than 35 years, but they have some dearths and disadvantages [12]:

- They ignore events shorter than 30 seconds. If the interval contains features from more than one Stage, it is scored as the Stage whose features have the longest duration.
- They are designated for healthy adult people and hence, it is not possible to score atypical patterns in cases of ill people or children.
- Some wave patterns (sleep spindles or K complexes) are not well defined, especially with respect to automated sleep scoring.

2.3 Cyclic alternating pattern

The alternation of the above defined sleep stages represents the macrodynamics of brain. In the concrete sleep Stage the level of arousal is assumed to be stable [13]. Different approach gives the idea of cyclic alternating pattern (CAP). CAP is a "periodic EEG activity of non-REM sleep, characterized by sequences of transient electrocortical events that are distinct from the background EEG activity and recur at up to 1 min intervals" [14]. CAP is functionally connected with fluctuation of arousal. CAP sequences occur in all stages 1, 2, 3 and 4 and in preference to sleep onset, after awakeness during sleep and before the transition

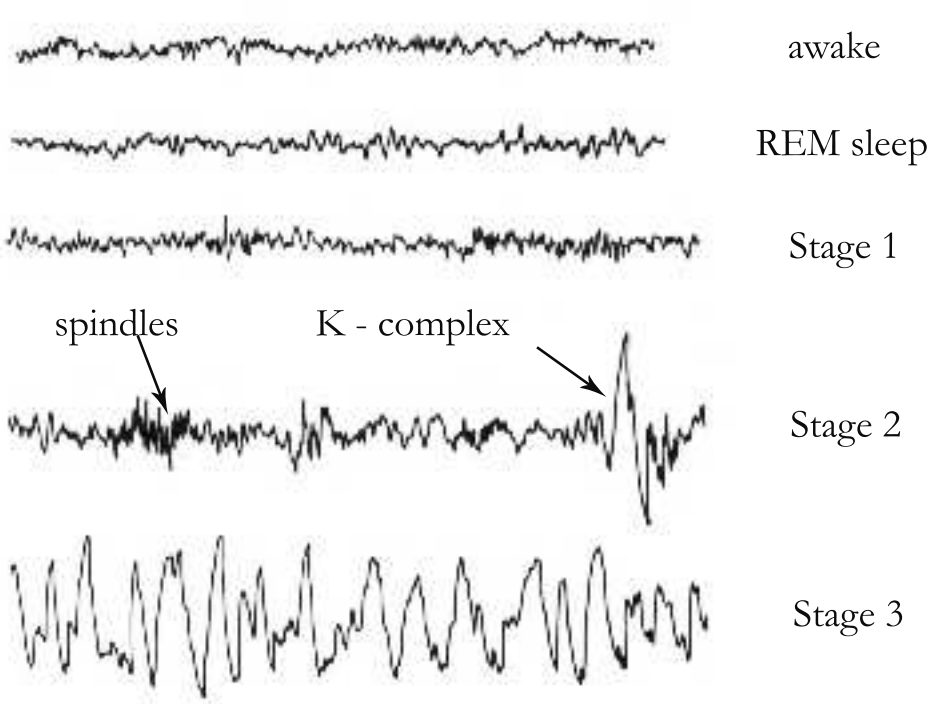

Figure 2.4: Wave pattern of different sleep Stages

from nonREM to REM sleep [13]. In normal REM sleep CAP does not occur. The rate time (CAP)/time(NREM) in young adults is about 23% and increases with age [13].

CAP is composed of two phases - phase A and phase B. At least two CAP cycles have to occur consecutively to be regarded as CAP sequence. Phase A represents events clearly outstanding from the background rhythm - abrupt changes in frequency and/or amplitude. Phase B is an intervening interval between phases A.

According to American Sleep Disorders Association CAP, sequences and microarousals may indicate instability or sleep disturbances with detrimental effects on sleep. Halász, Terzano et al. [15] presented an opposing idea : microarousals and CAP sequences are natural parts of the sleep texture. The physiological function of CAP could be protecting of reversibility of sleep and also in connection between the sleeping brain and his surrounding space to adapt to potential changes and danger.

2.4 Physiology of sleep

Sleep-wake cycle is regulated by multiple sleep and wake promoting systems, which are spread all over in the brain. Sleep begins with activation of the preoptic area of the anterior hypotha-

lamus. Sleep promoting neurons project to wake-promoting centres and inhibit them with γ-aminobutyric acid (GABA) as neurotransmitter. The inhibition of wake-promoting neurons works on other sleep-promoting neurons and activates them, which results in intensifying the sleep process [16].

REM sleep is regulated mostly by the brain stem; the two most important nuclei are laterodorsal (LDT) and pedunculopontine (PPT) tegmental nuclei. LDT and PPT project to thalamus, basal forebrain and the cortex, which output the desynchronized EEG pattern. The descending pathways to α motor neuron cause the skeletal muscle atonia [17]. Typical neuronal activity before the rapid eyes movements - PGO waves - rises from the pons and spreads through LGN (lateral geniculate nucleus) in thalamus to the occipital lobe [18, 17].

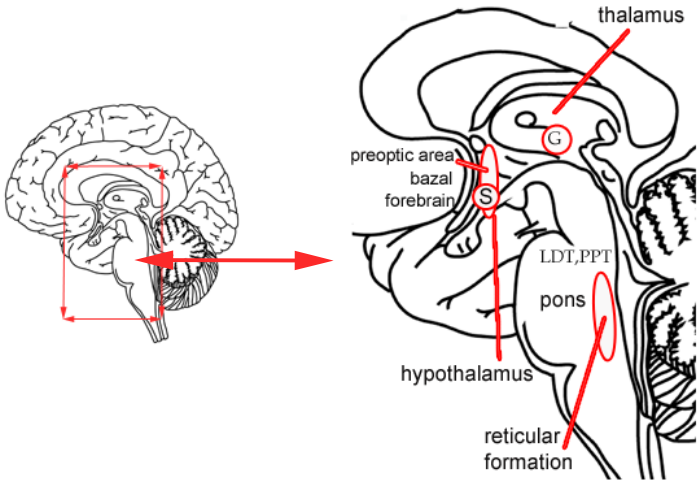

Figure 2.5: Sleep and waking centres. S - suprachiasmatic nucleus in hypothalamus, G - lateral geniculate nucleus in thalamus, LDT - laterodorsal tegmental nucleus, PPT - pedunculopontine tegmental nucleus, LDT, PPT in brain stem

The waking and arousal promoting centres are located in the posterior hypothalamus, basal forebrain, mesopontine tegmentum and contain cholinergic, noradrenergic, serotonergic and histaminergic neurotransmitters [16]. The arousal starts in reticular activating system (RAS), which receives collateral inputs from visceral, motor and sensory systems. RAS projects to the forebrain and cortex via thalamic and extrathalamic neural pathways.

2.5 Functions of sleep

For long time people were interested why sleep is so essential for the life. There are many theories that try to explain functions and the purpose of sleep. Some of them satisfactorily

interpret several facts, but broadly accepted theory that would explain all phenomena and experiments, does not exist till now. Here only the main theories are mentioned:

1. Conservation of energy: the main arguments for the purpose of sleep as reservation of energy are that during the sleep deprivation the energy consumption is increased and vice versa during sleep the basal metabolism is decreased about 5-25% [19].

2. Restoration of tissues and growth: during the first hours of sleep growth hormone excretion, cell mitosis and protein synthesis are increased. In the time of growth or after more laboured day the amount of NREM sleep is increased during the night. However J. Horne [20] criticized this theory. According to him cell mitosis occurs a few hours after food intake and has a circadian rhythm, the decreasing metabolic rate is in discrepancy with the protein synthesis that needs higher energy cost and the increased temperature of head after physical activity is the cause of increased rate of SWS.

3. Thermoregulation: in experiments with rats, long-term sleep deprived rats showed the temperature increased in about 10 degree [21], so sleep probably decreases the temperature.

4. Regulation of emotions [22]: in humans the sleep deprivation causes the disturbances of emotional behavior (such as concentration, interest for distinct goal, etc.), particularly SWS deprivation induces depressive or hypochondriacal states. So NREM sleep is likely to be involved in adjusting and regulating these emotions. This theory is supported by clinical observations that depressed patients show lower duration of NREM sleep as well as that metabolic rates and neuronal discharge are higher in brain regions that take control of emotions (limbic structures) during NREM sleep in contrast with waking state.

5. Neural maturation: one part of theories about sleep functions is concerned with REM sleep. The percentage of REM sleep of total sleep time decreases with age - in about 6. month of prenatal phase the children spend about 80% of sleep in REM sleep, but young adult people only 25% [19]. So it is assumed that during REM sleep the maturation of brain and myelinization of nerve fibers proceed.

6. Memory and learning: both types of sleep NREM and REM play a key role in memory consolidation and learning. There is an information transfer between cortex and hippocampus during the sleep that realizes the fixation of memory traces or during REM sleep the insignificant bindings are abolished [23]. With this reprocessing of information also the learning process is related. Several papers refer the improvement of

performance perceptual or motor task after sleep [24, 25]. The improvement is due to sleep and not due to time interval or circadian factors.

2.6 Models of sleep regulation

Today it is generally accepted that there are three processes that regulate sleep: a homeostatic process, a circadian process and an ultradian process [26].

The homeostatic process takes control of the amount of sleep and wakefulness, so that the homeostasis is reached. It increases the fatigue and sleep propensity during wakefulness and decreases it during sleep. The indicator of homeostatic process is SWS, which occurs more in the first part of sleep and its presence during the night gradually decreases. The SWS activity is significantly enhanced during the recovery night after sleep deprivation [27]. In contrast, daytime naps cause the attenuation of SWS [26]. Until now, physiological centre of the homeostatic process has not been identified.

Circadian process reflects the influence of external events which oscillate with circadian rhythm. Circadian process represents the alternation of sleep propensity with cca 24 hours rhythm. Also, some other processes show circadian behavior - for example the core body temperature, plasma melatonin or cortisol concentration [28]. In the forced desynchrony protocol the circadian and homeostatic processes can be unlike the homeostatic process, the brain structure of the circadian pacemaker is known - it is the suprachiasmatic nuclei of the hypothalamus [28] (see Fig 2.5).

Ultradian process administers the variation of nonREM and REM phases during the sleep.

One of the basic models is the two-process model of sleep regulation [29, 26]. It assumes the interaction of the homeostatic and circadian processes. The homeostatic variable S (sleep propensity) rises exponentially during wakefulness until it reaches the upper threshold H - the beginning of the sleep. During sleep, S decreases, untill it reaches the lower threshold L characteristic for the arousal. Both thresholds H and L change according to the phase of the day. The exponential function is fitted through 3 data points: the relative slow wave activity at the end of a normal night, after normal waking and after 40 hours of sleep deprivation.

Other models of sleep regulation propose variant interaction between homeostatic and circadian process or add other components, for review see [26].

Chapter 3

The Nature of Sleep EEG

Before application of some theory on data the nature of the signals and all assumption of that theory should be checked. The nature of EEG - if it is deterministic process or stochastic process - has been examined for several decades of years. For stochastic processes the spectral theory is used, which became widespread after the invention of the algorithm for fast Fourier transformation. The basic assumption in this theory is the stationarity of the signals.

Chaos (nonlinear) theory became popular after the Grassberger - Procaccia algorithm for computation of correlation dimension was published. For using chaos theory again the stationarity must be fulfilled and theoretically infinite amount of data should be available. The application of this theory on non-deterministic data can give strange results.

3.1 Linear approach

Spectral theory is conventional and the most used linear tool in the analysis of biosignals. Spectral analysis is used to investigate the signal's power in the various frequency bands and also the mutual relationships between more signals. It is based on Fourier transform, which displays signal in the frequency domain [30]:

$$C_k = \sum_{j=0}^{N-1} X_j e^{2\pi ijk/N} \qquad k = 0, ..., N-1, \tag{3.1}$$

where $X_1, ...X, x_i, ...X_N$ is the measured signal in the time domain, C_k is the amplitude corresponding to the k^{th} frequency and N is the number of values.

The power of particular frequency band is computed as the sum of modulus-square amplitudes belonging to this band. Here is an example of the power in alpha band (8 Hz-12 Hz):

$$P(\alpha) = \sum_{k=k_{8Hz}}^{k=k_{12Hz}} |C_k|^2, \tag{3.2}$$

where k_{8Hz} is the lower limit of alpha band and k_{12Hz} is the upper limit of alpha band.

Another often computed index is coherence; it reflects the degree of synchrony between signals from different derivations (brain areas). It is calculated as the ratio between cross-spectrum of two signals and a product of their autospectra:

$$coh_{AB}(f) = \frac{||P_{AB}(f)||^2}{P_A(f)P_B(f)}, \tag{3.3}$$

where P_{AB} is the cross-spectral density of signals A,B and P_A, P_B are the autospectral density of these signals.

The principal assumption for using spectral theory in stochastic processes is the stationarity of the process. This property is never exactly fulfilled in the case of EEG [31], but can be approximated on very short time intervals (several seconds). For more details about assumptions and algorithms from spectral theory see [30, 31]. Some results of applying spectral analysis to sleep EEG are incorporated in the Rechtschaffen and Kales rules for scoring sleep stages [11].

3.1.1 Spectral properties of EEG

Dumermuth et al. [32, 33] have computed power and coherence spectra of all-night sleep EEG. In accordance with their results the integrated power and integrated coherence (0.1-7.0 Hz and 7.1-12.0 Hz) increases during SWS with regard to wakefulness. During REM phase the power decreases, but the coherence between hemispheres increases or maintains at the same level and it is most evident in the biparietal area [32]. The average power in frequency band 0-6 Hz is maximal in Stage 4; in the band 6-10 Hz it is in Stage 4 or in the Stage 3; in 12-14 Hz band in Stage 2 and in the band 14-30 Hz it is in the Stage 1 [33]. The shape of power spectra is similar in every Stage - the higher power is in the lower frequencies and vice versa. The range of power, e.g. the difference between highest and lowest power, varies with stages, the lowest range is in Stage 1 (12-14 dB) and increases with the depth of sleep to Stage 4 (29-32 dB). In Stage REM the range of power is between Stages 1 - 2 and in waking it is similar as in Stage 1. Coherence in the low frequencies (0-8 Hz) is maximal in REM sleep, in the middle frequencies (8-14 Hz) in Stage 3 or 4 and in the highest frequencies (14-30 Hz) again in REM sleep, it is most pronounced between symmetrical intercoms derivations.

For illustration we have computed the power spectra from all sleep stages and wakefulness; data were from a free database (www.physionet.org/physiobank/database/sleep-edf), see Fig. 3.1, for more information see Figure 6.

Achermann et al. [34] have done more precise coherence analysis of sleep EEG. They have evaluated Stage-dependent and topographic-dependent (intrahemispheric, intercoms -

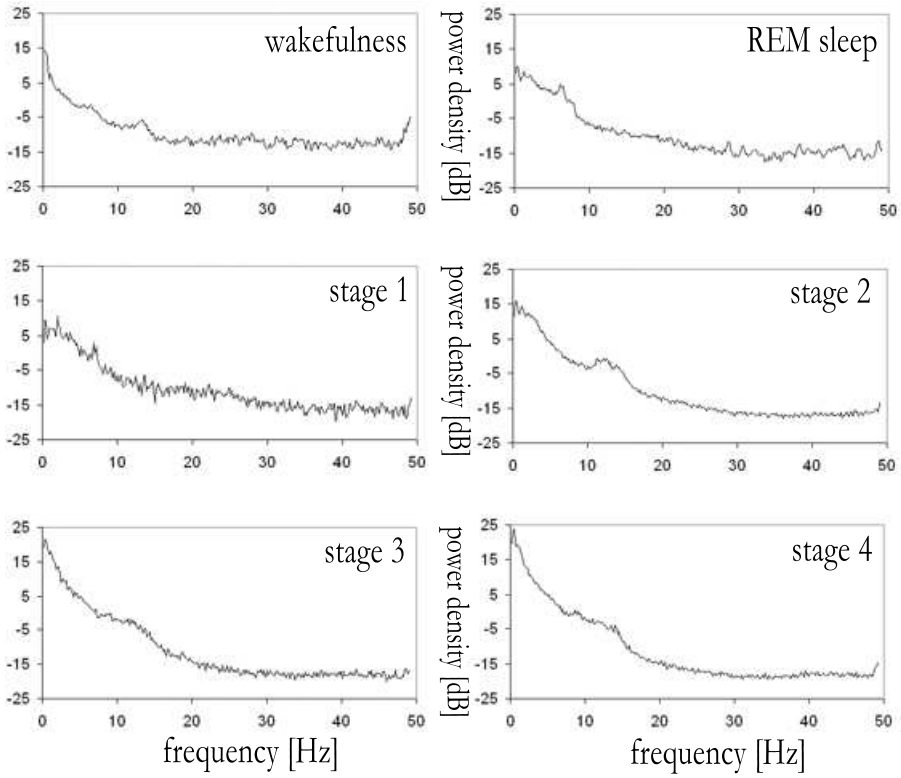

Figure 3.1: Power spectra density in different sleep stages and in wakefulness, the EEG derivation is Fpz-Cz, all signals are from the first episode of NREM-REM sleep cycle. 0dB = $1\mu V^2/0.25Hz$.
In the low-frequency part of the spectra (0-10 Hz) the maximal power is in the SWS, in the 12-14 Hz band the power is maximal in the Stage 2 and in the fast-frequency band the power is maximal in wakefulness.

homologous and non-homologous comparisons) coherence spectra. Coherence spectra between homologous derivations have declining frequency-dependent shape, in contrast with all other derivations with flat, low-level spectra. In NREM sleep the coherence spectra show outstanding peak in sigma band (13-14 Hz) in all derivations and smaller peaks in alpha and low delta bands. In coherence spectra in REM sleep these peaks are attenuated.

Merica and Blois [35] have compared the power in different frequency bands in NREM versus REM sleep episodes within sleep cycle as well as during the course of the night. Within NREM episode the power in β(14.75 Hz-30 Hz) band changes reciprocally to the slower bands (δ (0.5 Hz-3.75 Hz), θ (3.75 Hz-6.75 Hz)). In the last quarter before REM phase powers in all bands but β decreases and β power increases. The decrease of α (6.75 Hz-12.5 Hz), σ (12.5 Hz-14.75 Hz), θ and δ powers persists also on the first 30 % of time of REM phase and then the powers are stable. β power remains at the same level as in the end of NREM phase. The power of slower frequency bands (α, θ and δ) in NREM decreases during the night. Power

of delta band decreases in accordance with the homeostatic process. The evolution of beta and sigma powers during the night differ from the slower bands: after the second episode of NREM sleep their power increase. The course of powers of all bands in REM sleep is similar - it increases in all cases.

Ferri et al. [36] have focused on the analysis of high-frequency bands: β(15-25 Hz), $\gamma 1$ (25-35 Hz) and $\gamma 2$ (35-45 Hz). The powers in these frequency bands do not show significant changes, but the peaks of ratios of $\beta/\gamma 2$ and $\gamma 1/\gamma 2$ are highly correlated with occurrence of REM sleep, during the NREM phases these ratios decrease. The delta power displays reciprocal activity with these two ratios.

3.2 Chaos in EEG?

However, brain as the highest control system with many feedbacks appears to be a suitable object for nonlinear theory. Many methods of nonlinear theory are based on reconstruction of the phase space. According to Taken's theorem [37] it is possible to reconstruct a phase space topologically equivalent with the original one from a single observable variable. The reconstruction is done by time delay embedding (or related methods). From single variable X we obtain vectors in m-dimensional phase space:

$$\mathbf{x}_i = (X_i, X_{i-\tau}, X_{i-2\tau}, ..., X_{i-(m-1)\tau}), \tag{3.4}$$

where τ is the time delay, m is the embedding dimension. Since we have only limited amount of data, the proper choice of m and τ is crucial for the good reconstruction. The irregular nonperiodic time series that are nevertheless deterministic and are just slightly predictable are called chaotic time series. Two main properties of chaotic systems are self-similarity and sensitive dependence on initial conditions. These features can be treated by computing correlation dimension D_2 and Lyapunov exponent λ.

3.2.1 Complexity measures

First attempts to apply variables from nonlinear theory to EEG appeared after publication of the Grassberger-Procaccia algorithm (GPA) for computing the correlation dimension D_2. D_2 is a measure of a complexity of the system. For deterministic systems D_2 reaches finite values (sufficient embedding dimension must be specified), especially for chaotic systems it is noninteger value and for stochastic systems it is determined as high as the embedding dimension m. The finite estimate of D_2 determines the number of effective degrees of freedom of the deterministic dynamical system. GPA is based on computation of the correlation sum [38]:

$$C_2(\epsilon) = \frac{2}{(N)(N-1)} \sum_{i=0}^{N} \sum_{j>i}^{N} \Theta(\epsilon - \|\mathbf{x}_i - \mathbf{x}_j\|), \tag{3.5}$$

where $\mathbf{x}_i$, $\mathbf{x}_j$ are vectors in the phase space, N is the number of vectors and $\Theta(\epsilon - \|\mathbf{x}_i - \mathbf{x}_j\|))$ is the Heaviside function, which is equal one if the pair of vectors $\mathbf{x}_i$, $\mathbf{x}_j$ are less than a geometrical distance ϵ and zero otherwise. D_2 is defined as:

$$D_2 = \lim_{\epsilon \to 0} \lim_{N \to \infty} \frac{\ln C_2(\epsilon)}{\ln \epsilon} \tag{3.6}$$

C_2 is computed for several values of embedding dimension m. For deterministic signals $C_2(\epsilon)$ shows a power-law behavior, so if we take the local slope of $\ln C_2$ against $\ln \epsilon$, then the value of the plateau is taken as the estimate of D_2. In the case of EEG there are some factors which influence the exactness of the result: the number of the data, the signal to noise ratio and the stationarity of the data. It is necessary to find a compromise of the data size, which is of sufficient length, but the stationarity can be assumed.

Another characteristic, often used in analyses of physiological data, is the largest Lyapunov exponent λ - the measure of the exponential divergence of trajectories in the phase space [38]:

$$\delta_{\Delta n} \simeq \delta_0 e^{\lambda \Delta n}, \tag{3.7}$$

where δ_0 is the beginning distance between two close trajectories in the phase space and $\delta_{\Delta n}$ is this distance after Δ n time steps. Positive value of λ implies the presence of chaos behind the time series. Likewise as D_2, the precise value of λ is not easy to compute for EEG, there are the same sources of problems, including stationarity level and noise corruption.

In 1985, Babloyantz et al. [2] predicted the existence of the low-dimensional chaotic attractor in the sleep Stages 2 and 4 (for Stage 2, $D_2 = 5.03$, for Stage 4 D_2= 4.05, $\lambda \in (0.3, 0.8)$). Other results also conclude that D_2 in sleep are smaller than in awake EEG. D_2 seems to be highest in REM sleep and smallest in the Stage 4 [39, 1]. Similarly, the deeper the sleep, the lower the values of λ [40]. However, the finite estimates of D_2 of EEG were received with skepticism by many researchers from the area of nonlinear dynamics [1]. They pointed to some crucial details of the algorithm and assumptions, which may not hold (e.g. stationarity, the sufficient data size, proper embedding). Theiler et al. [41] have demonstrated that also for time series with autocorrelated Gaussian noise GPA gives spurious estimations of D_2 and proposed to omit those pairs of vectors which are closer than autocorrelation time. The re-examination of the previous results using this correction [42] showed that the low-dimensional estimate of D_2 in EEG was an artefact of the temporal autocorrelation.

3.2.2 Surrogate data

Another approach to investigate the nonlinear nature of signals is to compare them with surrogate data. Surrogate data are created by preserving one discriminatory property, while other properties are changed. It is a statistical test that aims at finding out whether the data from different classes of processes could give similar values of the chosen property [1]. If the nonlinearity of the signal is assumed, the null hypothesis is stated that it is linear stochastic process and a set of stochastic surrogate data is made. If the value of computed property of the original signal is significantly different from the values of surrogates, the null hypothesis can be rejected. In opposite case it is possible to look for a new discriminatory property. More information about surrogate data method can be find in [43, 1, 38].

In testing the surrogate data, D_2 does not appear to be the best discriminatory measure to distinguish between deterministic and stochastic nature of EEG [1]. Pereda et al. [4] have computed the fractal exponent γ and the D_2 of sleep stages using surrogate data in order to reveal whether finite estimates of D_2 are due to the nonlinear character of EEG, or whether EEG is better described as linearly-correlated noise. Fractal exponent γ is a measure used for fractal stochastic processes. Power spectra of stochastic signals can show power-low behavior with $1/f^{\gamma}$, where γ is the slope of linear fit of the power spectrum density in the double logarithmic graph. Following their results, only SWS displays nonlinear structure (D_2 of original EEG differs significantly from surrogate data), EEG spectra of the Stages 1, 2 and REM sleep show a frequency power-low dependence $1/f^{\gamma}$ with γ between 1 and 3. For γ it holds the more complex signal the lower value of γ. Between γ and D_2 there is a negative linear relationship in Stages 1, 2, REM and in wakefulness. Both indexes relates to the complexity of signal, however γ is preferable to D_2 due to its less time demanding computation.

Olbrich et al. [44] used autoregressive modeling of EEG during sleep and surrogate testing. The null hypothesis of linearly correlated noise has to be rejected if less than 2 % of segments have length of 1s for every Stage of sleep. As a consequence of nonstationarity, the percentage of rejection rose with the length of segments.

For detection of mutual relationship between more signals nonlinear methods can be used as well. Pereda et al. [45] have applied multivariate nonlinear time series analysis to investigate the interdependencies between channels C3/A2 and C4/A1 during all sleep stages. The results were very sensitive to used parameters, the significance of results were checked by surrogate data. According to their results the interdependencies between these channels increased with depth of sleep and were mostly of linear type.

3.2.3 Usefulness of nonlinear measures in sleep EEG

The question whether EEG is deterministic or chaotic is still open, although the chance that the process behind EEG is low-deterministic is small. However, nonlinear measures could be beneficial in effort to find appropriate variables for characterizing and describing various psychophysiological states of the brain. Today it is not expected the number of differential equations needed to describe EEG from the values of D_2; it is interpreted as a measure of the system's "complexity".

Fell, Rőschke et al. [3] used several spectral and nonlinear measures in order to find the best variables for discriminating the sleep stages. The best discrimination is achieved with the combination of spectral entropy, λ, entropy of amplitudes, D_2 and spectral edge. If the number of variables is limited to 2 or 3, the lowest error is obtained by combining λ, entropy of amplitudes and D_2. Complexity measures related to the concept of entropy rates estimation were reported by Rosipal [46] as appropriate indicators in classification of brain states. This suggest that nonlinear measures may offer additional information about the brain state.

Chapter 4

Time Series Prediction

The sources of predictability in time series can be of two origins [38]: linear correlations and determinism. Linear correlations are traditionally modeled with stochastic processes such as MA (moving average), AR (autoregressive) or ARMA (the combination of both processes above). Here is the most general ARMA model:

$$X_{n+1} = \sum_{i=0}^{M} a_i X_{n-i} + \sum_{i=0}^{N} b_i \eta_{n-i}, \tag{4.1}$$

where M, N are the orders of the processes and η_i are Gaussian uncorrelated random increments.

In deterministic approach the transition from one state of the system to another follows a rule:

$$\mathbf{x}_{n+1} = \mathbf{f}(\mathbf{x}_n) \tag{4.2}$$

where $\mathbf{x_n}$, $\mathbf{x_{n+1}}$ are vectors in the state space and can be approximated with vectors embedded after Takens theorem, see 3.4. Then the forecast of the measured signal is:

$$X_{n+1} = \mathbf{F}(\mathbf{x}_n) = \mathbf{F}(X_i, X_{i-\tau}, X_{i-2\tau}, ..., X_{i-(m-1)\tau}), \tag{4.3}$$

where $\mathbf{F}(\mathbf{x_n})$ is composed of the measurement function (here the state vectors are made with time delayed copies of the measured signal) and the transitional rule. Prediction is close connected with modeling - first a model of the dynamics is made and then measured values and the model are used to make the prediction. If the process behind the dynamics is unknown information about it should be obtained from the data. The data used to be divided into training set, where the parameters of the predictor are determined, and a testing set. The adequacy of the model and the accuracy of predictions used to be evaluated with the error

(or cost) function, e.g.:

$$e = \sqrt{\frac{1}{N}\sum_{n=1}^{N}(X_{n+1} - \mathbf{F}(\mathbf{x}_n))^2}, \tag{4.4}$$

where X_{n+1} is the true continuation of signal, $\mathbf{F}(\mathbf{x}_n)$ is the predicted value and N is the number of points in testing set.[1] The predictability of the signal is good if the error function gives low values for long time. There are several measures that can evaluate the predictability of the signal: mostly used are normalized prediction error $e/StDev(X)$, where e is the error function and $StDev(X)$ is the standard deviation of the predictable sample of the signal; predictive time - time up to which the error function is lower than a certain threshold [5], correlation coefficient between observed and predicted time series [47], and etc. As the chaotic systems are sensitive to initial conditions, the average divergence of initially close trajectories is exponential (it is characterized by Lyapunov exponents). This implicates the limitation of time, on which these systems can be predicted and that the prediction error increases exponentially with time.

For forecasting several (τ) time steps ahead direct estimate from the training set can be made or the resultant value is achieved iteratively [48]:

$$X_{n+\tau} = \mathbf{F}(\mathbf{x}_{n+\tau-1}) = \mathbf{F}(\mathbf{F}(\mathbf{x}_{n+\tau-2})) = ... = \mathbf{F}^{\tau}(\mathbf{x}_n) \tag{4.5}$$

4.1 Local predictors

Local models are based on the assumption that close states in the phase space will evolve similarly in the future at least on a short part of their trajectories. The most simple local predictor [49, 38] finds the nearest neighbour of the predicted point in the phase space and follows its trajectory. On a short part of the trajectory this could work well, but as it is just copying of the past states, later it would produce a cyclic orbit. An improvement of prediction can be achieved by using an averaged image of several nearest neighbors or neighbours which are stationed into a neighbourhood of a given diameter.

The utilization of nearest neighbours is a common feature of local methods. It is important to choose reasonable value of the neighbourhood's diameter [38]: it should contain enough neighbours to "give a good statistics", but it can not be too big in order all neighbours be close states to the predicted vector. Also the diameter should exceed the amplitude of noise, otherwise the algorithm catches the dynamics of the noise and not the process behind the data. Local methods used to give good results if the data base is big and the level of noise is small.

[1] In some technique the minimization of the error function is used to compute the parameters of the model in the training set

Next way how to use neighbourhood's relationship is to make local approximation of the dynamics. Farmer and Sidorowich [50] and Sauer [51] used the local linear approximation in their algorithm. To predict $X(t+T)$ a metric on the state space is assigned and the k nearest neighbours $\mathbf{x}(t')$ of the vector $\mathbf{x}(t)$ are chosen, so that they minimize the distance $||\mathbf{x}(t) - \mathbf{x}(t')||$. Then the linear polynomial is fitted with least square method between the pairs - neighbour $\mathbf{x}(t')$ and its real continuation in time $X(t'+T)$:

$$\mathbf{F}(\mathbf{x}) = \mathbf{a}\mathbf{x}(\mathbf{t}) + b, \tag{4.6}$$

where $\mathbf{a}$ is d - dimensional vector and b is scalar, the mapping is from d-dimensional space into one-dimensional. For the local approximation of the dynamics also other models than linear can be used, e.g. polynomial with higher degree, radial basis functions, and etc.

4.2 Global predictors

Global predictors make direct modeling of the function $\mathbf{F}$ on the whole attractor.

The functional form of $\mathbf{F}(\mathbf{x})$ is often requested as a linear combination of some basis functions:

$$\mathbf{F}_M(\mathbf{x}) = \sum_{m=1}^{M} c_m \Phi_m(\mathbf{x}), \tag{4.7}$$

where c_m are coefficients and $\Phi_m(\mathbf{x})$ is the set of basis functions. Basis functions are fixed and only the coefficients are varied in order the error function becomes minimal. Traditionally polynomials can be chosen as the basis set, however the number of parameters to be fitted increases with the order of the polynomial l and the embedding dimension d as $\approx d^l$ [50].

Giona [52] has overcome this problem of multiparameter optimization with the measure - based approximation of function $\mathbf{F}(\mathbf{x})$; valid for ergodic systems. $\mathbf{F}(\mathbf{x})$ is expressed as linear combination of polynomials, which are orthogonal with respect to the invariant (natural) measure μ_I:

$$\int_{\mathcal{C}} \Phi_i(\mathbf{x})\Phi_j(\mathbf{x}) d_{\mu_I} = \delta_{ij}, \tag{4.8}$$

where $\Phi_i(\mathbf{x})$, $\Phi_j(\mathbf{x})$ are polynomials in $\mathbf{x}$, δ_{ij} is Kronecker tensor, $\mathcal{C}$ is the limit set on which the natural measure is concentrated. Invariant measure can be defined as the probability that the system is found in the concrete subset of the attractor [1]. The corresponding invariant density can be expressed as:

$$\rho(\mathbf{x}) = \frac{d\mu_I(\mathbf{x})}{d\mathbf{x}} \approx \frac{1}{N} \sum_{k=1}^{N} \delta^d(\mathbf{x} - \mathbf{y}(k)), \tag{4.9}$$

where δ^d is d-dimensional Dirac function and N is the number of attractor's points. The

polynomials can be obtained iteratively in the Gram-Schmidt orthogonalization process, with setting $\Phi_1(\mathbf{x}) = 1$. The coefficients c_m can be determined by [53]:

$$c_m = \int \mathbf{F}(\mathbf{x})\Phi_m\rho(\mathbf{x})d^dx = \frac{1}{N}\sum_{k=1}^{N}\mathbf{F}(\mathbf{y}(k))\Phi_m(\mathbf{y}(k)) = \frac{1}{N}\sum_{k=1}^{N}\mathbf{y}(k+1))\Phi_m(\mathbf{y}(k)) \quad (4.10)$$

because $\mathbf{y}(k+1) = \mathbf{F}_M(\mathbf{y}(k))$.

Another often used method is radial basis functions method [54, 55, 38]. In this method finite number of vectors in R^d are chosen as the radial centres and the distances of $\mathbf{x}_n$ to all centres are computed. Then the predictor is looked for in the form of linear combinations of scalar functions:

$$\mathbf{F}(\mathbf{x}) = \lambda_0 + \sum_{i=1}^{N_c}\lambda_i\mathbf{\Phi}(||(x) - \mathbf{x}_i^c||), \quad (4.11)$$

where $\mathbf{x}^c$ are the radial centres, N_c is the number of the radial centres, $||.||$ is the Euclidean norm, $\mathbf{\Phi}(||.||)$ are the radial functions, and λ_i are coefficients to be determined. Typical radial basis functions are $\Phi(r) = r$, r^3, $\sqrt{r^2+c}$,$1/\sqrt{r^2+c}$, and $e^{-r^2/c}$, where c is a constant [55]. If the centres and inherent parameters of the scalar functions are fixed, the coefficients λ_i can be determined in least-squeares method on the training set. In dependence on the number of the radial basis centers this method can be considered as global ($N_c \approx$ number of points in the training set) or as a local method (when several nearest centers to $\mathbf{x}_n$ are taken into account). The centres can be chosen randomly, uniformly distributed through the phase space or with respect to the invariant measure.

4.3 Prediction algorithms used on EEG

The practical importance of forecasting in human EEG can be in catching of some processes and predicting events that potentially endanger the life such as sleep onset during driving a car, beginning of epileptic seizure, etc. However, prediction algorithms can be used not only if the interest is in future values of time series, but also in investigating the dynamics of signals. The more predictable signal is, the higher degree of deterministic structure contains [6].

Andrzejak et al. [56] have investigated the nature and the complexity of EEG signal during various conditions: healthy subjects with eyes open/closed and intracranial EEG from epilepsy patients during a seizure and during seizure free intervals. They computed correlation dimension D_2, prediction error from simply averaged image of 5 nearest neighbours and tested the results with surrogate data method. The null hypothesis of linear stochastic process was rejected for both D_2 and prediction error for epileptic seizure. In contrast EEG of healthy subjects with open eyes confirmed the null hypothesis in both measures.

Brandt et al. [57] have applied two prediction algorithms - k -nearest neighbours local linear approximation (KNNLLA) and global linear AR modeling - to study the human Alpha EEG activity. First they tested both algorithms on Hénon and Mackey-Glass systems with various level of additive noise, and sine wave with Gaussian noise. KNNLLA showed better prediction ability than AR model in Hénon map and Mackey-Glass system with moderately level of noise, however, in high level of noise KNNLLA was not better than AR. In stochastic sine wave system with Gaussian noise KNNLLA was not better than AR also with a small amount of noise. EEG was taken from subjects during relaxation with and without eyes closed. After their results, the prediction error was higher for KNNLLA than AR for all tested data, and it resembled rather the results obtained for noisy sine wave. They inherited from this that EEG is rather stochastic in the nature.

Hernández et al. [5] have used weighted local linear approximation algorithm. They supposed that non-linear forecasting methods are more appropriate for EEG signals. Various segments of EEG show big variability in the prediction quality. In their work EEG segments from Alfa activity were divided into three groups after this prediction ability: 1. unpredictable (the quality of prediction is satisfactory till 50 ms) 2. predictable between 50 ms - 250 ms 3. very predictable on more than 250 ms. The very predictable segments visually correspond to well-organized alpha pattern (the sharp peak in alpha band appears in power spectrum and in no other frequencies), and vice versa - the unpredictable group corresponds to desynchronized alpha activity (in power spectrum besides the alpha peak other frequencies have considerable contributions.)

Aftanas et al. [6] have detected the differences in the dynamics of various emotions with nonlinear prediction algorithm (local linear approximation). EEG during negative evoked emotions showed better predictability than neutral or positive emotions. The predictability was evaluated due to correlation coefficient between forecasted and real values in testing set.

Chapter 5

Data

Data with all-night polysomnographic records were kindly provided by Prof. G. Dorffner, received by The Siesta Group Schlafanalyse GmbH. The records were obtained from 20 healthy subjects, 10 men and 10 women. Ages ranged from 23 to 82 years old with an average 50 ± 21.5 years. EEG derivations are: Fp1-M2, C3-M2, O1-M2, Fp2-M1, Fp2-M1, C4-M1, O2-M1, M1-M2, see 2.2, and M1, M2 are the left and right mastoids. Precise numbers of sleep stages and standard characteristics derived from hypnograms are in Table 5.1. Numbers of sleep stages (30s records) are in the first column; data in the second column are the average values over 20 subjects related to total sleep time, the beginning of sleep is set as the first appearance of the sleep Stage 2. Sleep efficiency is the ratio of time spent in Stages 1-4 or REM sleep to the whole sleep time, where also movement time and some awakenings during the night are included; in sleep medicine this parameter discriminates some sleep disorders.

EEG is sampled with 256 Hz and filtered (HP: 0.1 Hz, LP: 75 Hz, filter: 50 Hz). Sleep stages are scored by two independent judges, when there was an ambiguity, third independent judge decided.

total	18107	sleep efficiency [%]	91.6	±	6.2
waking	2069	% waking	8.0	±	6.2
Stage1	1452	% Stage 1	7.8	±	3.5
Stage2	7860	% Stage 2	45	±	7.3
Stage3	1586	% Stage 3	9.3	±	4.3
Stage4	1865	% Stage 4	10.9	±	2.7
REM sleep	3226	% REM sleep	18.4	±	3.6
Movement time	110	% Movement time	0.5	±	0.6

Table 5.1: Numbers of sleep stages (first column) and sleep efficiency and average percentage of sleep stages during the sleep (mean ± standard deviation).

Second group of data came from a relaxation experiment, which was performed in our laboratory [58]. 8 healthy subjects were trained in relaxation during 25 sessions. Four subjects overslept several times. 3 min. long EEG from 6 channels was recorded, EEG derivations were: C3P3, C4P4, F3C3, F4C4, P3O1, and P4O2 after international 10-20 electrode placement system, see 2.2 for EEG measurement. EEG was sampled at 500 Hz and filtered from 0,75 Hz. After subjective scoring the records were selected into two groups: records of sleep onset (36 files) and records of relaxation state (339 files).

Chapter 6

Preliminary results and Plan

Till now only data from the relaxation experiment were processed. The ability of two complexity measures correlation dimension D_2 and fractal exponent γ to discriminate the subtle changes in human EEG during relaxation and sleep onset was compared [59]. Correlation dimension was computed after (GPA), see 3.2.1. Fractal exponent γ was found to be negatively correlated with D2, so for less complex signal D2 shows lower value and γ higher value [60, 4].

The whole mean of D_2 over all subjects and EEG derivations for relaxed data was 4,41 $\pm$ 0,6 and for sleep onset data D_2 was equal 3,95 $\pm$ 0,46. In the same way, γ for relaxed data was 2,24 $\pm$ 0,34 and for sleep onset signals γ was equal 2,59 $\pm$ 0,21. Both measures indicated that brain was less complex system during sleep onset than during the relaxation.

With regard to topographic characteristics of brain all files were sorted after the derivation of EEG. D_2 and γ averaged over signals with the same EEG derivation are in the Table 6.1. The highest difference between relaxation and sleep onset appeared in the occipital area (especially in p4o2) for both D_2 and γ. For γ the relative change in absolute value was higher than for D_2 in all derivations, therefore γ appeared to be more sensitive and hence more appropriate for discriminating these states of brain.

With the aim to reveal possible intersubject differences D_2 and γ was averaged over all channels for individual subject. Interesting findings were observed; subjects with tendency to oversleep (four subjects) showed lower D2 during relaxation than subjects that had never overslept. Subjects were divided into two subgroups after this tendency to oversleep, the averaged value of D2 and γ for these two subgroups are in Table 6.2. Within the subgroup with the tendency to oversleep the hypothesis that D2 shows higher values during relaxation (wakefulness) than during sleep onset was confirmed in 2 subjects from 4; alpha was lower in relaxation than in sleep onset in 3 subjects from 4.

Furthermore the ability of D_2 and γ to catch the process of sleep onset was examined. The EEG data were visually scored for sleep onset markers and compared with the behavior of D_2 and γ computed for EEG fragmented into 10 equal epochs. In most cases, observed features

	C3P3		C4P4		F3C3		F4C4		P3O1		P4O2	
	γ	D_2	γ	D_2	γ	D_2	γ	D_2	γ	D_2	γ	D_2
Relax.	2,35	4,28	2,33	4,33	2,23	4,46	2,26	4,41	2,16	4,43	2,12	4,53
Sleep	2,56	4	2,57	3,99	2,55	4,29	2,55	4,07	2,46	3,95	2,58	3,88
Rel.D.	-9,03	6,58	-10,24	7,78	-14,22	3,77	-12,47	7,7	-13,69	10,82	-21,48	14,27

Table 6.1: Topographical characteristics of D_2 and γ.
Relax. - relaxation state, Sleep - sleep onset, Rel.D. - relative deviation, which was computed as $100 * (Relax. - Sleep)/Relax$

	Relaxation		Sleep onset	
	D_2	γ	D_2	γ
Tendency to oversleep	4,04 $\pm 0,46$	2,45 $\pm 0,21$	3,95 $\pm 0,46$	2,59 $\pm 0,21$
No tendency to oversleep	4.68 ± 0,46	2,09 ± 0,24	-	-

Table 6.2: Mean and standard deviation of D_2 and γ for subgroups of subjects with and without the tendency to oversleep.

of sleep onset were the reduction of alpha activity - the change from continuous alpha to alternation of epochs with alpha activity and epochs with decreased amplitude of and mixed frequency EEG. Both indexes were sensitive to these changes.

The obtained results demonstrated that originally assumed lower complexity during sleep onset in contrast to complexity in relaxation was not so obvious. If only subjects with the tendency to oversleep were taken into account D_2 did not show significantly different values between relaxation and sleep onset, γ supported the hypothesis in 3 subjects from 4. The interpretation can be that relaxation and light sleep are very close states of brain dynamics or that for sleep onset detection longer time than three mins is needed. The unusual differences in D_2 and γ between subgroups with and without tendency to oversleep were confronted with the ability to improve the relaxation during the training process (25 sessions). Several authors found that long-term averaged decrease of D_2 was a sign of improving relaxation [47]. In this study the tendency not to oversleep was highly correlated with higher trend in improving the relaxation.

Both measures D_2 and γ were applied also on data from free database of physiologic signals (www.physionet.org/physiobank/database/sleep-edf), signals were from all-night polysomnographic recordings (horizontal EOG, FpzCz and PzOz EEG, each sampled at 100 Hz) from 4 healthy subjects (21-35 years old). Segments 1.5-5 min long from sleep onset process - wakefulness, Stage 1, and Stage 2 - were chosen. However, the signals were too corrupted with noise and it was impossible to calculate D_2.

From this database also 5-20 epochs (30 s long) long segments from all sleep stages and wakefulness were chosen and the power spectrum density was calculated, see Figure 3.1.

In the next work the dynamics of sleep EEG will be investigated with nonlinear prediction algorithms; the larger database of all-night records with scored sleep stages will be used. Several works [4] have reported the deterministic character of deep sleep, so best predictability is supposed to be in this state.

In current research, big effort is spent on developing new systems suitable for automated scoring of sleep stages. As the hypothesis is that the deep sleep is better predictable with nonlinear methods than with some classical stochastical algorithm, but for Stages 1, 2, and REM sleep this does not hold, we will attempt to develop a classificator for sleep stages based on various predictability for various sleep stages.

The progress of the work will be as follows:

- To check the ability of D_2, γ, and other suitable measures from [58] to detect and predict sleep onset on the big database received by The Siesta Group Schlafanalyse GmbH.
- To investigate nonlinear prediction algorithms and examine their properties on classical dynamical systems such as Lorenz system, Henon system, Mackey - Glass system with various amount of additive noise.
- To find the most optimal nonlinear prediction algorithm for sleep EEG, adjust parameters of the algorithm concretely for various sleep stages. The discriminatory ability between sleep stages will be considered. All results should be compared with a traditional stochastical prediction.
- To apply the final algorithm to another kind of data - such as electrocardiogram or financial data.

Bibliography

[1] A. Galka. *Topics in Nonlinear Time Series Analysis*. World Scientific, 2000.

[2] A. Babloyantz and J. M. Salazar. Evidence of Chaotic Dynamics of Brain Activity During the Sleep Cycle. *Phys. Lett. A*, 111:152–156, 1985.

[3] J. Fell, J. Rőschke, K. Mann, and C. Schaffner. Discrimination of sleep stages: a comparison between spectral and nonlinear EEG measures. *Electroencephalogr. Clin. Neurophysiol.*, 98:401–410, 1996.

[4] E. Pereda, A. Gamundi, R. Rial, and J. González. Non-linear behaviour of human EEG: fractal exponent versus correlation dimension in awake and sleep stages. *Neuroscience Letters*, 250:91–9, 1998.

[5] J. L. Hernández, R. Valdés, et al. EEG predictability: adequacy of non-linear forecasting methods. *Int. J. of Bio-Medical Computing*, 38:197–206, 1995.

[6] L. I. Aftanas, N. V. Lotova, et al. Nonlinear Forecasting Measurements of the Human EEG During Evoked Emotions. *Brain Topography*, 10:155–162, 1997.

[7] M. Moráň. *Praktická elektroencefalografie*. IDVPZ Brno, 1995.

[8] A.L. Loomis, E.N. Harvey, and G.A Hobart. Cerebral States During Sleep, as Studied by Human Brain Potentials. *J. Exp. Psychol.*, 21:127–144, 1937.

[9] E. Aserinsky and N. Kleitman. Regularly Occuring Periods of Eye Motility, and Concomitant Phenomena, During Sleep. *Science*, 118:273–274, 1953.

[10] W.C. Dement and N. Kleitman. Cyclic Variations in EEG During Sleep and their Relation to Eye Movements. Body Motility and Dreaming. *Electroencephalogr. Clin. Neurophysiol.*, 9:673–390, 1957.

[11] A. Rechtschaffen, A. Kales, and (Eds.). *A Manual of Standardized Terminology, Techniques and Scoring System for Sleep Stages of Human Subject*. US Government Printing Office, National Institute of Health Publication, Washington DC, 1968.

[12] S.-L. Himanen. *A New Visual Adaptive Scoring System for Sleep Recordings.* Electronic dissertation, Acta Electronica Universitatis Tamperensis, 61, 2000.

[13] M. G. Terzano, L. Parrino, and M. C Spaggiari. The cyclic alternating pattern sequences in the dynamic organisation of sleep. *Electroencephalogr. Clin. Neurophysiol.*, 69:437–447, 1988.

[14] M. G. Terzano et al. Altas, rules, and recording techniques for the scoring of cyclic alternating pattern (CAP) in human sleep. *Sleep Medicine*, 2:537–553, 2001.

[15] P. Halász, M. G. Terzano, L. Parrino, and R. Bódisz. The nature of arousal in sleep. *J. Sleep Res.*, 13:1–23, 2004.

[16] K. Sakai and S. Crochet. A neural mechanism of sleep and wakefulness. *Sleep and Biological Rhythms*, 1:29–42, 2003.

[17] WWW. Sleep Study URL: http://www.sleepstudy.org.

[18] H. L. Atwood and W. A. MacKay. *Essentials of Neurophysiology.* B.C. Decker Inc, 1989.

[19] S. Nevšímalová, K. Šonka, et al. *Poruchy spánku a bdění.* Maxdorf/Jessenius, Praha, 1997.

[20] J. Horne. The Phenomena of Human Sleep. *Karger Gazette*, 1997.

[21] A. Rechtschaffen and J. M. Siegel. *Sleep and Dreaming. In: Principles of Neuroscience. Edited by E. R. Kandel, J. H. Swartz and T. M. Jessel.* McGraw-Hill, New York, 2000.

[22] Zi-Jian Cai. The Function of Sleep: Further Analysis. *Physiology Behavior*, 50:53–60, 1989.

[23] R. Stickgold. Sleep: off-line memory reprocessing. *Trends in Cognitive Sciences*, 2, No. 12:484–492, 1998.

[24] R. Stickgold, James L. T., and J. A. Hobson. Visual discrimination learning requires sleep after training. *Nature Neurosci.*, 3:1237–1238, 2000.

[25] R. Huber, Ghilardi M.F., M. Massimini, and G. Tononi. Local sleep and learning. *Nature*, 430 (6995):78–81, 2004.

[26] P. Achermann and A. A. Borbély. Mathematical Models of Sleep Regulation. *Frontiers in Bioscience*, 8:683–693, 2003.

[27] A. A. Borbély, F. Baumann, D. Brandeis, I. Strauch, and D. Lehmann. Sleep Deprivation: Effect on Sleep Stages and EEG Power Density in Man. *Electroencephalogr. Clin. Neurophysiol.*, 51:483–493, 1981.

[28] Ch. Cajochen and D. J. Dijk. Electroencephalographic activity during wakefulness, rapid eye movement and non-rapid eye movement sleep in humans: Comparison of their circadian and homeostatic modulation. *Sleep and Biological Rhythms*, 1:85–95, 2003.

[29] S. Daan, D. G. M. Beersma, and A. A. Borbély. Timing of human sleep: recovery process gated by a circadian pacemaker. *Am. J. Physiol.*, 246:161–178, 1984.

[30] W. H. Press et al. *Numerical Recipes in C.* Cambridge University Press, 1988.

[31] A. S. Gevins and A. Rémond. *Handbook of Electroencephalography and clinical Neurophysiology. Methods of Analysis of Brain Electrical and Magnetic Signals.* Elsevier, Amsterdam, 1987.

[32] G. Dumermuth and D. Lehmann. EEG Power and Coherence during Non-REM and REM Phases in Humans in All-Night Sleep Analyses. 1981.

[33] G. Dumermuth, B Lange, D. Lehmann, et al. Spectral Analysis of All-Nigth Sleep EEG in Healthy Adults. *European Neurology*, 22:322–339, 1983.

[34] P. Achermann and A. A. Borbély. Coherence analysis of the human sleep electroencephalogram. *Neuroscience*, 85:1195–1208, 1998.

[35] H. Merica and R. Blois. Relationship between the time courses of power in the frequency bands of human sleep EEG. *Neurophysiol Clin*, 27:116–128, 1997.

[36] R. Ferri, M. Elia, S. A. Musumeci, and S. Pettinato. The time course of frequency bands (15-45 Hz) in all-night spectral analysis of sleep EEG. *Clinical Neurophysiology*, 111:1258–1265, 2000.

[37] F. Takens. *Detecting strange attractors in fluid turbulence. In D. Rand and L.S. Young, editors, Dynamical systems and turbulence.* Springer, Berlin, 1981.

[38] H. Kantz and Schreiber T. *Nonlinear Time Series Analyses.* Cambridge University Press, 1997.

[39] T. Kobayashi, K. Misaki, et al. Non-linear analysis of the sleep EEG. *Psychiatry and Clinical Neurosciences*, 53:159–162, 1999.

[40] J. Rőschke, J. Fell, and P. Beckmann. The calculation of the first positive Lyapunov exponent in sleep EEG data. *Electroencephalogr. Clin. Neurophysiol.*, 86:348–352, 1993.

[41] J. Theiler. Spurious dimension from correlation algorithms applied to limited time-series data. *Phys. Rev. A*, 34:2427–2432, 1986.

[42] J. Theiler and P. E. Rapp. Re-examination of the evidence for low-dimensional, nonlinear structure in the human electroencephalogram. *Electroencephalogr. Clin. Neurophysiol.*, 98:213–222, 1996.

[43] T. Schreiber and A. Schmitz. Surrogate time series. *Physica D*, 142:346–382, 2000.

[44] E. Olbrich, P. Achermann, and P. F. Meier. Dynamics of human sleep EEG. *Neurocomputing*, 52-54:857–862, 2003.

[45] E. Pereda, R. Rial, Gamundi A., and J. Gonzáles. Assessment of changing interdependencies between human electroencephalograms using nonlinear methods. *Physica D*, 148:147–158, 2001.

[46] R. Rosipal. *Kernel-Based Regression and Objective Nonlinear Measures to Assess Brain Functionnig, PhD thesis.* University of Paisley, Scotland, 2001.

[47] L. Aftanas and S. Golocheikine. Non-linear dynamic complexity of the human EEG during meditation. *Neuroscience Letters*, 330:143–146, 2002.

[48] L. Smith. Does a Meeting in Santa Fe Imply Chaos? *In: Weigend, A. S. and Gershenfeld, N. A. and (Eds.):Time Series Prediction: Forecasting the Future and Understanding the Past*, pages 323–343, 1993.

[49] A. S. Weigend, N. A. Gershenfeld, and (Eds.). *Time Series Prediction: Forecasting the Future and Understanding the Past.* Santa Fe Institute Studies in the Science of Complexity, Proc. Vol. XV, Addison-Wesley, 1993.

[50] J. D. Farmer and J.J. Sidorowich. Predicting Chaotic Time Series. *Phys. Rev. Letters*, 59:845–848, 1987.

[51] T. Sauer. Time Series Prediction by Using Delay Coordinate Embedding. *In: Weigend, A. S. and Gershenfeld, N. A. and (Eds.):Time Series Prediction: Forecasting the Future and Understanding the Past*, pages 175–193, 1993.

[52] M. Giona, F. Lentini, and V. Cimagalli. Functional reconstruction and local prediction of chaotic time series. *Phys. Review A*, 44, No. 6:3496–3502, 1991.

[53] H. D. I. Abarbanel. *Analysis of Observed Chaotic Data*. Springer, 1996.

[54] M. Casdagli. Nonlinear prediction of chaotic time series. *Physica D*, 20:335–356, 1991.

[55] L. A. Smith. Identification and prediction of low dimensional dynamics. *submitted to Neuroscience Letters*, Physica D, 1992.

[56] R. G. Andrzejak, K. Lehnertz, et al. Indications of nonlinear deterministic and finite-dimensional structures in time series of brain electrical activity: Dependence on recording region and brain state. *Phys. Rev. Letters*, 64, 061907:1–8, 2001.

[57] M. E. Brandt, A. Ademoğlu, and W. S Pritchard. Nonlinear Prediction and Complexity of Alpha EEG Activity. *International Journal of Bifurcation and Chaos*, 10, No. 1:123–133, 2000.

[58] M. Teplan, A. Krakovská, and S. Štolc. EEG Responses to Long-term Audio-Visual Stimulation. *International Journal of Psychophysiology*, submitted.

[59] K. Šušmáková. Complexity of EEG During Sleep Onset Process . *MEASUREMENT SCIENCE REVIEW*, 2005.

[60] A. Krakovská and S. Štolc. Spectral decay vs. correlation dimension of EEG. *submitted to Neuroscience Letters*, 2005.